Electrochimica Acta 194 (2016) 187–198

Contents lists available at ScienceDirect

Electrochimica Acta

journal homepage: www.elsevier.com/locate/electacta

Electroanalysis of formetanate hydrochloride by a cobalt phthalocyanine functionalized multiwalled carbon nanotubes modified electrode: characterization and application in fruits

Francisco Wirley Paulino Ribeiro[a], Francisco Willian de Souza Lucas[a], Lucia H. Mascaro[a], Simone Morais[b,*], Paulo Naftali da Silva Casciano[c], Pedro de Lima-Neto[c], Adriana N. Correia[c]

[a] LIEC, Departamento de Química, Universidade Federal de São Carlos, Rodovia Washington Luis km 235, Caixa postal 676, 13560-970 São Carlos, SP, Brazil
[b] REQUIMTE/LAQV, Instituto Superior de Engenharia do Instituto Politécnico do Porto, Rua Dr. António Bernardino de Almeida 431, 4200-072 Porto, Portugal
[c] GELCORR, Departamento de Química Analítica e Físico-Química, Centro de Ciências, Universidade Federal do Ceará, Bloco 940 Campus do Pici, 60455-970 Fortaleza, CE, Brazil

ARTICLE INFO

Article history:
Received 9 September 2015
Received in revised form 9 February 2016
Accepted 15 February 2016
Available online 18 February 2016

Keywords:
Multiwalled carbon nanotubes
metal phthalocyanine complexes
modified electrode
pesticides

ABSTRACT

This study characterizes the electroanalytical behavior of the carbamate pesticide formetanate hydrochloride (FMT) at a cobalt phthalocyanine (CoPc) functionalized multiwalled carbon nanotubes (*f*MWCNT) modified glassy carbon electrode (CoPc-*f*MWCNT/GCE). Nafion® was used to improve solubility and dispersibility of *f*MWCNT. The construction of the developed electrode was characterized by high-resolution field-emission gun scanning electron microscopy, Raman spectroscopy, cyclic voltammetry and electrochemical impedance spectroscopy. FMT exhibited a behavior consistent with a three-step reaction of the electrochemical-chemical-electrochemical mechanistic type at CoPc-*f*MWCNT/GCE (three anodic peaks at 0.26, 0.55 and 1.2 V, and two cathodic peaks at 0.35 and 0.50 V *vs.* Ag/AgCl/3 M KCl). Highly reproducible and well-defined peaks were obtained at the optimum experimental conditions (Britton-Robinson buffer at pH 5.0, accumulation potential 1.55 V, accumulation time 5 s, frequency 100 s^{-1}, amplitude 30 mV, and scan increment 3 mV). Peak currents were found to be proportional to the FMT concentrations in the range of 9.80×10^{-8} to 3.92×10^{-6} mol dm^{-3} with a detection limit (LOD) of 9.7×10^{-8} mol dm^{-3}. The modification of GCE with CoPc-*f*MWCNT enhanced the electrocatalytic activity and provided high sensitivity (3.51 A mol^{-1} dm^3). The developed electroanalytical methodology was successfully applied to FMT residue analysis in mango and grape samples with recoveries in the range of 94.2 ± 4.5 to 105.7 ± 1.8%. The proposed electroanalytical approach represents a reliable, sensitive and environmental friendly analytical alternative for determination of FMT.

1. Introduction

Current concerns of the deleterious environmental and health impacts of carbamate pesticides have been increasing. Humans and other non-target species are exposed to residues of these cholinesterase-inhibiting chemicals via nutritional sources (legumes, fruits, contaminated meat, dairy products, *etc.*), water and/or through environmental/occupational settings [1]. As a member of the N-methyl carbamate class of chemicals, formetanate hydrochloride (3-dimethylaminomethyleneaminophenyl methylcarbamate hydrochloride; FMT) shares the common mechanism of toxicity. It is a miticide/insecticide registered for use on several fruits (grapefruit, lemon, lime, nectarine, orange, tangelo, tangerine, *etc.*) and nonagricultural uncultivated areas/soils [2]. In this context, the development of electrochemical devices is a key tool for implementation of rapid, sensitive, versatile, environmental friendly, *in situ* real-time and cost-effective residues screening programs [3]. Moreover, electrochemical sensors can also provide information regarding kinetic and mechanistic aspects of degradation [4–6].

Nanostructured carbon materials have proved to be very interesting in various research fields due to their inherent advantages such as excellent electrical conductivity, high-surface to volume ratio, significant mechanical strength, good chemical stability and pore structure [7–11]. The use of Nafion® to improve solubility and dispersibility of multiwalled carbon nanotubes

* Corresponding author. Tel.: +351 228340500; fax: +351 228321159.
E-mail address: sbm@isep.ipp.pt (S. Morais).

http://dx.doi.org/10.1016/j.electacta.2016.02.086
0013-4686/

(MWCNT) has provided a useful avenue for preparing MWCNT-based sensors [12]. In addition, MWCNT decorated with transition metal phthalocyanine complexes (MPc) hold great promise for designing new sensing platforms [13–17]. Phthalocyanine are 18 π-conjugated aromatic macrocycles that present remarkable optical and electrical properties, structural versatility and exceptional stability. Metal atoms (*e.g.* Co, Fe, Ni, and Cu) can be incorporated in the central region of the macrocycle to tailor some of their chemico-physical properties [18,19]. In particular, CoPc have the ability of undergoing fast redox processes, with minimal reorganizational energies, and can act as electron transfer mediator for several compounds. The immobilization of CoPc on suitable substrates can lead to modified electrodes with electrocatalytic properties [20]. In biosensor design, such as cholinesterase modified electrodes, CoPc were indicated as one of the most suitable for the detection of thiol-containing molecules [21], and has been used as electronic mediator to decrease the applied potential (from *ca.* 410 to 100 mV *vs.* Ag/AgCl), hindering the oxidation of other compounds thus reducing the interferences [22]. Enzymes were successfully immobilized on CoPc modified electrodes by entrapment in a photocrosslinkable polymer (PVA-AWP) [23,24]. Scarce studies have demonstrated the potential of MPc-MWCNT systems to improve the sensitivity of modified electrodes for pesticides (asulam, carbaryl, glyphosate and metolcarb) analysis [11,25–28] mostly in (tap/natural) waters and synthetic aqueous solutions [11,25–27]. Novel electrocatalytic platforms based on CoPc integrated with MWCNT for electroanalysis of pesticides in food commodities need clearly to be further explored. No electrochemical method based on MPc-MWCNT modified electrode for FMT detection was found in the literature so far, nor any mechanistic proposal involving its oxidation and reduction. FMT electroanalysis was only reported in four works [29–32]. FMT reduction was characterized at the dropping mercury electrode [29]. More recently, FMT was indirectly quantified by three different enzymatic biosensors [30–32]. However, the developed biosensors presented limited specificity since other pesticides from the carbamates family may also inhibit the enzymatic catalysis. Also, modified electrodes with biological components are more difficult to work with and less robust (to pH, temperature, applied potential, storage, etc.) [26].

Therefore, the main aims of this work were: i) to explore the advantages of combining CoPc and functionalized MWCNT solubilized in Nafion® (*f*MWCNT) for modification of glassy carbon electrode (GCE), ii) to develop and optimize a rapid, simple, accurate and low-cost sensitive electrochemical approach for FMT analysis based on the modified electrode (CoPc-*f*MWCNT/GCE), and iii) to propose a mechanism for the electrochemical behavior of FMT. The preparation of CoPc-*f*MWCNT/GCE was fully characterized by high resolution field-emission gun scanning electron microscopy (FEG-SEM), Raman spectroscopy, cyclic voltammetry (CV) and electrochemical impedance spectroscopy (EIS). Considering that real sample applications of electrochemical devices are rare, the performance of CoPc-*f*MWCNT/GCE for FMT quantification in fruits was also assessed. The chosen fruit species are those that have the lowest (0.02 mg kg^{-1} in mango) and the highest (1.0 mg kg^{-1} in grapes) established Brazilian FMT maximum residue limits (MRLs) [33].

2. Experimental

2.1. Reagents

Formetanate hydrochloride (certified purity higher than 99.6%), CoPc (97% purity), Nafion® (10 wt. % in H_2O) and pristine MWCNT (O.D. × L 6–9 nm × 5 μm, >95%) were purchased from Sigma–Aldrich (Steinheim, Germany). Standard solutions of FMT were prepared daily by dissolving an accurately weighed amount in ultrapure water. Britton-Robinson buffer (BR, 0.04 mol dm^{-3}) was prepared by mixing 0.04 mol dm^{-3} of phosphoric, acetic and boric acid. All other chemicals were of analytical grade. The ultrapure water (18.2 MΩ cm) was produced by a Milli-Q system (Millipore, Molsheim, France).

2.2. Electrode pretreatment and modification

Firstly, the functionalization of 500 mg of pristine MWCNT was carried in a 250 mL mixture of H_2SO_4:HNO_3 (3:1; v/v) with magnetic stirring at 26 ± 1 °C for 4 h [34–36]. The *f*MWCNT were filtered through a 0.45 mm Nylon filter membrane (Millipore, Molsheim, France), washed with ultrapure water, and dried in oven at 70 °C for 12 h [26,34–36].

Prior to the modification, the GCE (geometric area of 0.0314 cm^2 Metrohm, The Netherlands) was polished with 3.0 μm diamond paste slurry, rinsed with ultrapure water, cleaned ultrasonically in acetone and water alternatively for 3 min, and then dried with nitrogen. 1 mg of *f*MWCNT plus 1 mg of CoPc were dispersed by ultrasonic stirring for 30 min in 1 mL of dimethylformamide (DMF) containing 0.5% Nafion® (DMF/Nafion® 0.5%). Next, 0.5 μL of the CoPc-*f*MWCNT suspension was dropped on the cleaned GCE surface, and dried at 26 ± 1 °C for 1 h. The other tested electrodes, i.e., 0.5% Nafion®/GCE (modified with DMF/Nafion® 0.5%), MWCNT/GCE (modified with MWCNT dispersed in DMF/Nafion® 0.5%) and *f*MWCNT/GCE (modified with functionalized MWCNT dispersed in DMF/Nafion® 0.5%) were prepared similarly.

Surface characterization of the modified GCE was accomplished by FEG-SEM using a FEG-Zeiss model Supra 35-VP (Carl Zeiss, Germany). Raman spectroscopy assays of the several tested modifications (MWCNT, *f*MWCNT and CoPc–*f*MWCNT prepared as described above) were carried out on a Horiba Jobin Yvon model HR550 spectrometer using the 514.5 nm excitation line from an argon ion laser ion.

2.3. Electrochemical studies

Electrochemical experiments were performed with a potentiostat/galvanostat, AUTOLAB model PGSTAT 30 (Metrohm-Eco Chemie, The Netherlands) controlled by a computer through the Model NOVA version 1.9 software. A conventional electrochemical cell consisting of an Ag/AgCl/3 M KCl reference electrode, a platinum plate as the auxiliary electrode, and 0.5% Nafion®/GCE, MWCNT/GCE, *f*MWCNT/GCE, CoPc-*f*MWCNT/GCE as working electrode were used. CV and square wave-voltammetry (SWV) experiments were carried out in 0.04 mol dm^{-3} BR buffer (pH 5.0) over the potential range of 0.0 to 0.8 V or 0.0 to 1.5 V. The optimal SWV parameters were: accumulation potential (E_{acc}) 1.55 V, accumulation time (t_{acc}) 5 s, frequency (*f*) 100 s^{-1}, amplitude (*a*) 30 mV and scan increment (ΔE_s) 3 mV. EIS assays were performed in the presence of 1.0×10^{-3} mol dm^{-3} $Fe(CN)_6^{3-}$/$Fe(CN)_6^{4-}$ (1:1) in 0.1 mol dm^{-3} KCl at a frequency range of 10^{-1} to 6×10^4 s^{-1} and amplitude perturbation 5 mV. All measurements were carried out, at least, in triplicate.

2.4. Application to fruits

Fruit samples were acquired from local supermarkets at Fortaleza (Brazil). Samples of mango and grape were taken, chopped and homogenized in accordance with the guidelines of the European Council Directive [37]. Pesticide extraction was performed by the Quick, Easy, Cheap, Effective, Rugged and Safe – QuEChERS method [31,38,39]. An aliquot of 15 g of homogenized sample was quantitatively transferred to a QuEChERS tube containing the buffer–salt mixture 6 g magnesium

sulfate/1.5 g sodium chloride/1.5 g sodium citrate dehydrate (UCT, Bristol, USA). Next, 15 mL of acetonitrile were added and the QuEChERS tube was shaken vigorously during 3 min. After centrifugation in a QUIMIS® Q222T204 centrifuge (São Paulo, Brazil) for 5 min at 4500 rpm, the solvent layer was reduced to 2 mL by evaporation under vacuum in a QUIMIS® Q344M2 rotary evaporator (São Paulo, Brazil). Then, it was transferred onto a column cleanup (containing 150 mg magnesium sulfate, 150 mg primary secondary amine sorbent UCT Enviro-Clean Bristol, PA), shaken and centrifuged as mentioned above. The supernatant was then evaporated to dryness with a gentle stream of nitrogen. Immediately before electroanalysis, the residue was re-dissolved with the supporting electrolyte (10 mL of BR buffer, pH 5.0). Validation of the pesticide residue methodology was performed by recovery assays of fortified mango and grape samples at four spiking levels (0.13–0.73 mg kg^{-1} (w/w)). Blanks (non-spiked) and

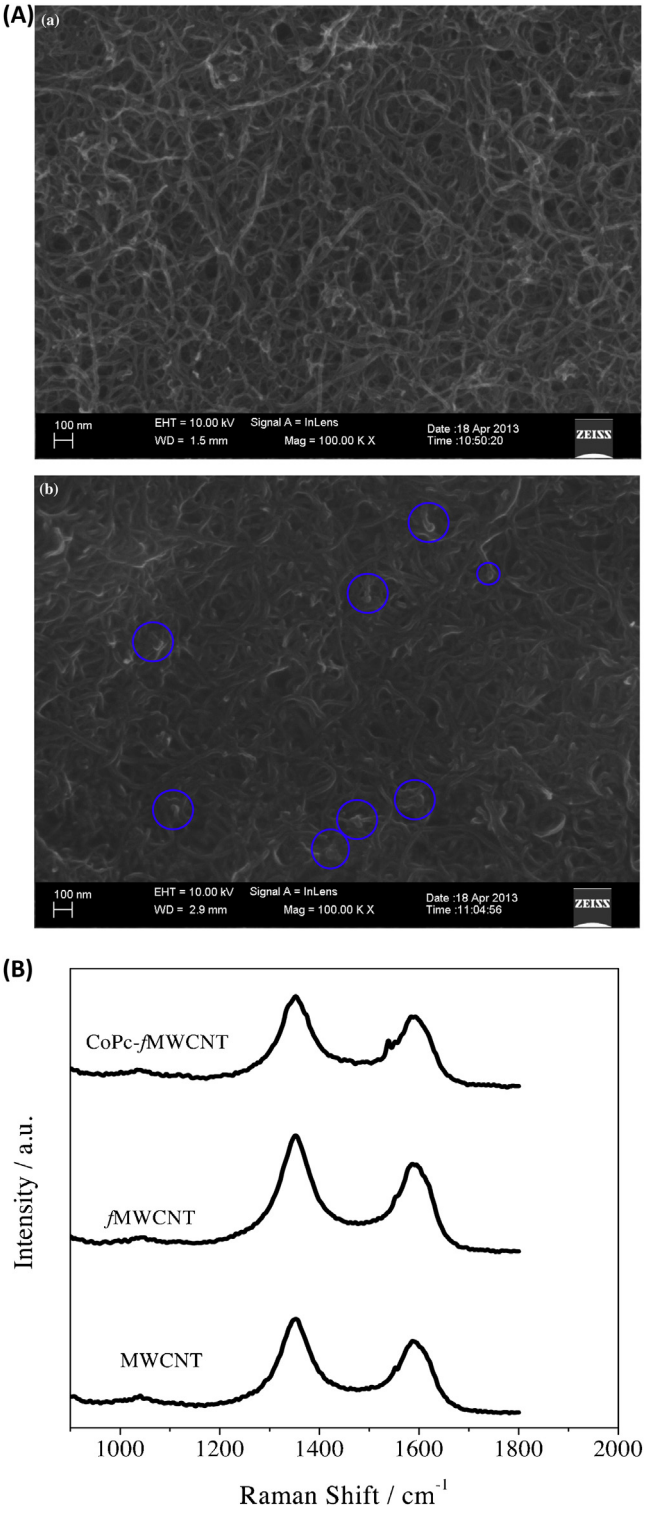

Fig. 1. (A) FEG–SEM images of (a) *f*MWCNT and (b) CoPc–*f*MWCNT; (B) Raman spectra of pristine MWCNT, *f*MWCNT and CoPc–*f*MWCNT.

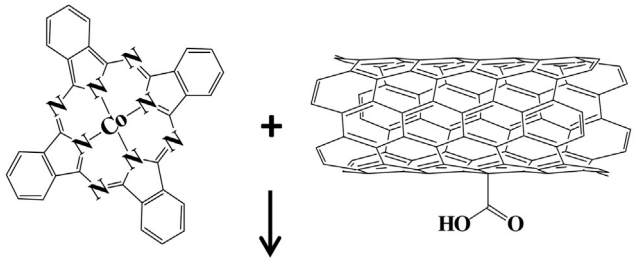

a) π - π interaction

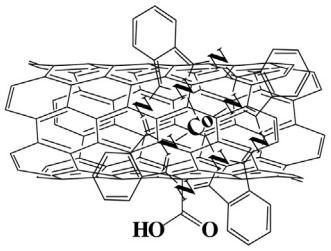

b) Coordinate bond c) Hydrogen bond

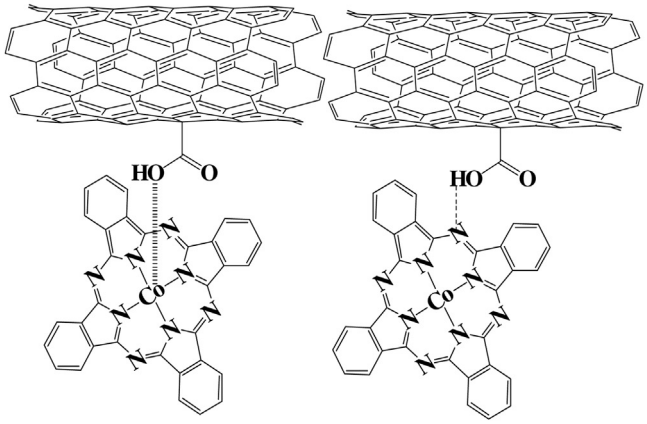

Scheme 1. Schematic representation of the interfacial interaction between *f*MWCNT and CoPc.

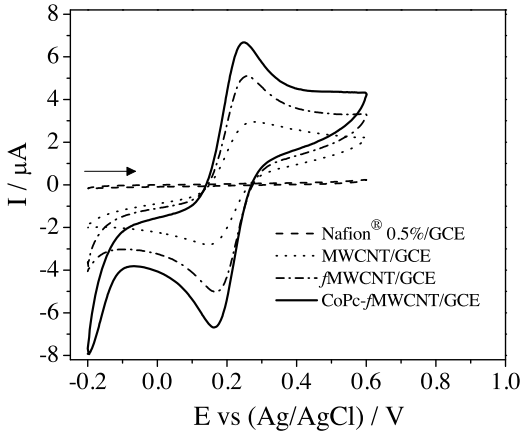

Fig. 2. Comparative cyclic voltammograms of 1.0×10^{-3} mol dm^{-3} $Fe(CN)_6^{3-}$/$Fe(CN)_6^{4-}$ (1:1) in 0.1 mol dm^{-3} KCl at 0.5% Nafion®/GCE, MWCNT/GCE, *f*MWCNT/GCE and CoPc–*f*MWCNT/GCE. Scan rate of 50 mV s^{-1}.

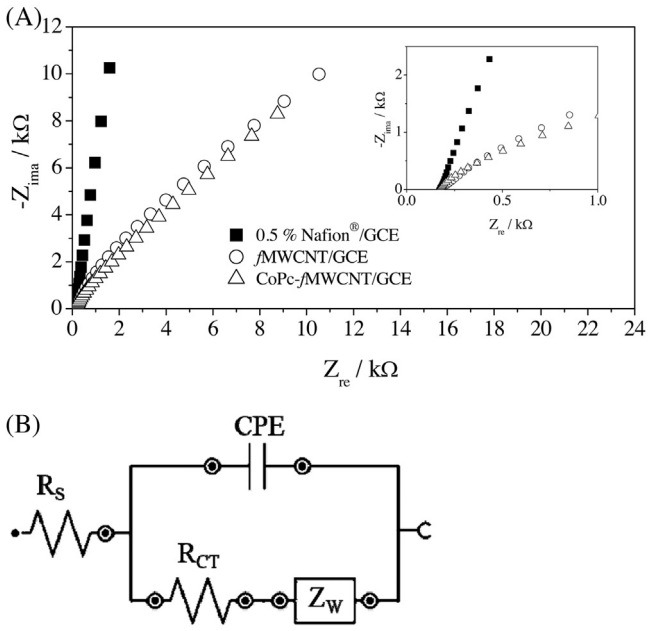

Fig. 3. (A) Nyquist plot of electrochemical impedance spectroscopy for the different modified electrodes for a frequency range of 10^{-1} to $6 \times 10^{4}\,s^{-1}$ and amplitude perturbation of 5 mV using 1.0×10^{-3} mol dm^{-3} $Fe(CN)_6^{3-}/Fe(CN)_6^{4-}$ (1:1) in 0.1 mol dm^{-3} KCl. (B) Equivalent electrical circuit comprising the resistance of the solution (Rs/Ω), the Warburg impedance (Zw/Ω), the double-layer capacitance (CPE/F), and the electron transfer resistance (Rct/Ω).

samples used for recovery assays were free of FMT residues. All measurements were carried out in triplicate by the standard addition method.

3. Results and discussion

3.1. Construction of CoPc-fMWCNT/GCE

3.1.1. Characterization of MWCNT, fMWCNT and CoPc-fMWCNT

FEG-SEM was used to evaluate the morphology of the pristine MWCNT, *f*MWCNT and CoPc-*f*MWCNT films. The typical morphology of the well-aligned MWCNT [40] was observed before and after functionalization (Fig. 1A a)). Based on FEG-SEM observations, the determined diameters were approximately 24 and 15 nm for MWCNT and *f*MWCNT, respectively. The detected decrease was due to rupture of nanotubes which also promoted the increase of edge planes. The presence of edge planes will promote the electrochemical reactions rates at the nanoscale [41]. The existence of functional groups on the sidewall of the MWCNT facilitated the modification with the charge transfer mediator (CoPc). The FEG-SEM image of CoPc-*f*MWCNT (Fig. 1A b)) shows a homogeneous and compact film; the entangled metal clusters can be clearly seen (blue circle in Fig. 1A b)) which is in agreement with previous related studies [26,42,43].

The functionalization of the carbon surface with carboxylic, alcohol, and ketone functional groups with predominance to carboxylic groups [41,44], and the interaction between *f*MWCNT and the CoPc were evaluated by Raman spectroscopy (Fig. 1B). Samples exhibited two characteristics peaks at 1350 cm^{-1} (D band) and at 1586 cm^{-1} (G band). The first one was due to Raman-active A_{1g} mode derived from the disordered carbon and defects of MWNT, as well as sp^3 hybridized carbon atoms, and the second band can be

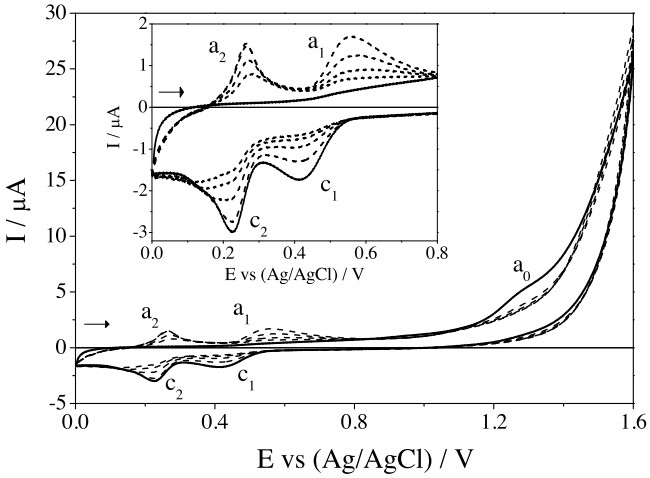

Fig. 4. Cyclic voltammograms of 1.0×10^{-5} mol dm^{-3} FMT (Britton-Robinson buffer pH 5.0) at CoPc-*f*MWCNT/GCE. Scan rate of 50 mV s^{-1}; first (solid line) and subsequent (dashed line) scans.

attributed to the Raman-active E_{2g} mode due to sp^2 hybridized carbon atoms in the graphene sheets of the carbon nanotubes [45]. The presence of the D and G bands before and after functionalization proved that the MWCNT structure was preserved. The D band intensity (I_D) was higher in the *f*MWCNT than in MWCNT evidencing the insertion of the functional groups in carbon nanotubes [46]. Frequently, the intensity ratio, I_D/I_G, is applied to analyze the structural aspects such as the ratio sp^3/sp^2 hybridized carbon atoms and amount of defects in carbon nanotubes. The attained I_D/I_G values were 1.277 and 1.282 for MWCNT and *f*MWCNT, respectively, suggesting that the attachment of functional groups occurred preferentially in the pre-existing defects of the carbon nanotubes. The slight diminution of the I_D/I_G ratio to 1.234 when CoPc were combined with *f*MWCNT can be attributed to non-covalent interaction [47]. The interfacial interactions of CoPc with *f*MWCNT (Scheme 1) comprises π-π type interaction, coordination bond between the cobalt atoms of the phthalocyanine complexes and the oxygen atoms of *f*MWCNT, and hydrogen bond between the nitrogen atoms of CoPc and hydrogen atoms of *f*MWCNT [48]. π-π stacking interactions (between CoPc and *f*MWCNT) have been reported to be the main ones when Nafion® is used to improve the solubility and dispersibility of *f*MWCNT [49,50].

3.1.2. Electrochemistry of CoPc-fMWCNT/GCE

The electrochemical properties of the electrode after the different modifications were firstly investigated by CV in 1.0×10^{-3} mol dm^{-3} $Fe(CN)_6^{4-}/Fe(CN)_6^{3-}$ (1:1) in 0.1 mol dm^{-3} KCl (Fig. 2). Nafion® acts as a polymer backbone to give stable and homogeneous films at the modified electrode with MWCNT (functionalized or not) [51]. The response of 0.5% Nafion®/GCE was very poor when compared with the other electrodes due to electrostatic repulsion between Nafion® and the $Fe(CN)_6^{3-}/Fe(CN)_6^{4-}$ redox probe. The peak currents clearly increased with the subsequent modifications with MWCNT or *f*MWCNT (*f*MWCNT/GCE > MWCNT/GCE >> 0.5% Nafion®/GCE), and CoPc (CoPc–*f*MWCNT/GCE > *f*MWCNT/GCE). Functionalization enhanced the charge transfer reaction. "Wrapping" of MWCNT or *f*MWCNT in Nafion improved their solubility without impairing their electrocatalytic properties. Such behavior has been demonstrated for other redox processes [12]. Since the walls of MWCNT are built up by π electrons delocalization from sp^2 hybrid orbital, delocalization of π bond can be formed in *f*MWCNT due to the carboxyl groups [52]. This phenomenon improved electron transport, hence increasing the current signal. Another cause is that edge planes present an enhanced catalytic activity in comparison to the basal planes, so *f*MWCNT (broken nanotubes) exhibited superior electrocatalysis activity [41,53]. The anodic-to-cathodic peak separation (ΔE_p) decreased with functionalization of MWCNT and non-covalent attachment of CoPc on the *f*MWCNT. The obtained ΔE_p values were 137.9 ± 4.2, 92.6 ± 1.1 and 83.9 ± 3.1 mV for MWCNT/GCE, *f*MWCNT/GCE and CoPc-*f*MWCNT/GCE, respectively, reflecting the high impact of the modification on the reversibility of the charge-transfer reaction.

EIS was also applied since it is an effective tool for the characterization of the interface properties of the electrode surface

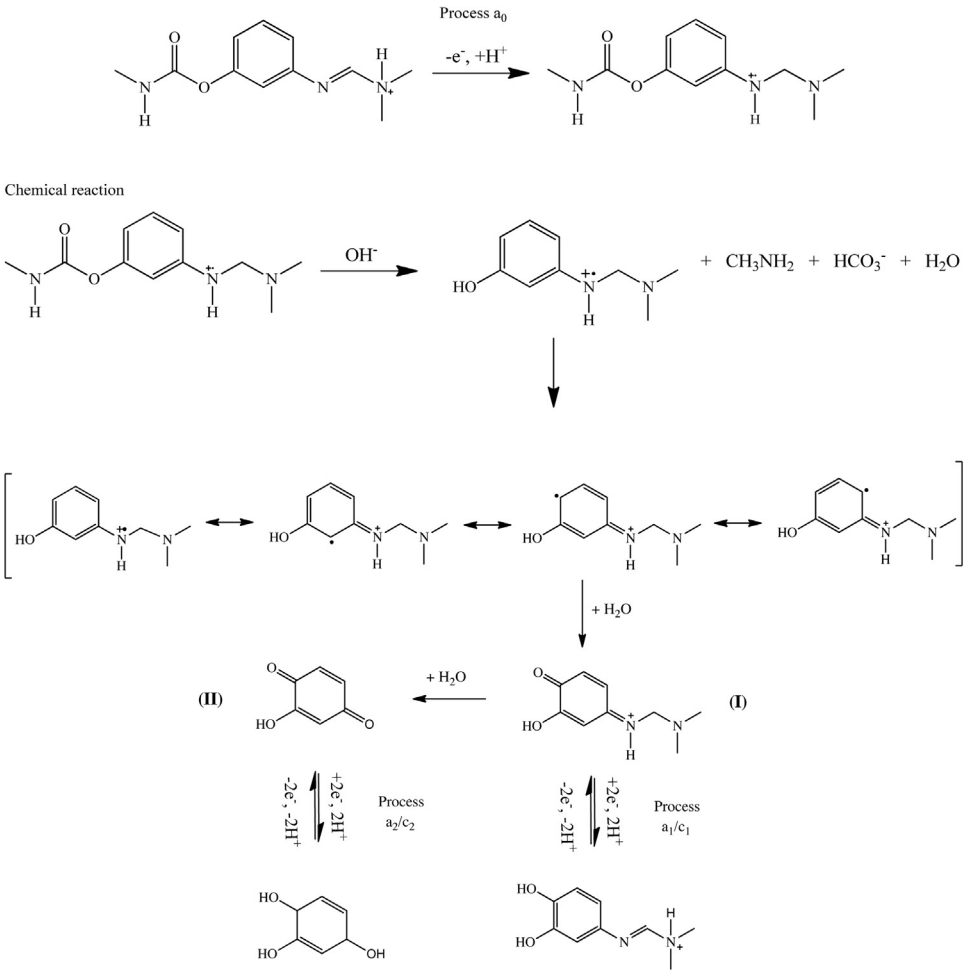

Scheme 2. Proposed electrochemical-chemical-electrochemical mechanism for FMT at CoPc-*f*MWCNT/GCE.

during different modification steps. The attained Nyquist diagrams at the 0.5% Nafion®/GCE, *f*MWCNT/GCE and CoPc-*f*MWCNT/GCE are exhibited in Fig. 3A. The equivalent electrical circuit used to fit the electrochemical impedance data is also presented in Fig. 3B. The results are in agreement with those attained by CV (Fig. 2). Nyquist plot of 0.5% Nafion®/GCE exhibited the higher charge transfer resistance (Rct/Ω) because the negatively charged Nafion® hampered the diffusion of $Fe(CN)_6^{3-}/Fe(CN)_6^{4-}$ towards the active sites of the electrode surface. Additionally, the calculated slope of the Bode plot (log $|Z|$ *vs* log f (ac-frequency)), −0.9, was very close to the theoretical value (−1.0) expected for true capacitors [54]. After modification of the electrode with *f*MWCNT or CoPc-*f*MWCNT, the Nyquist plots included a semicircle at high frequency region and a linear relationship at low frequencies. At higher frequencies, the diameter of the semicircular portion is equal to the R_{ct} which controls the electron transfer kinetics of the redox process at the electrode interface. At lower frequencies, the linear part is typical of a mass diffusion-limited electron-transfer process. The observed R_{ct} of the CoPc-*f*MWCNT/GCE (7.98 ± 0.63 kΩ) was lower than the one obtained for *f*MWCNT/GCE (12.13 ± 0.56 kΩ) confirming that the CoPc-*f*MWCNT film improved the conductivity and facilitated electron transfer.

The influence of the electrode surface modification in the apparent electron transfer rate constant (k_{app}) was evaluated using the equation (1):

$$k_{app} = RT(n^2F^2AR_{ct}C)^{-1} \quad (1)$$

where R is the ideal gas constant ($J\,mol^{-1}\,K^{-1}$), T is the temperature (K), n is the number of electrons involved in reaction (n = 1), F is the Faraday constant ($C\,mol^{-1}$), A is the electrode area (cm^2), R_{ct} is the charge transfer resistance (Ω) and C is the concentration of the redox species ($mol\,cm^{-3}$) [55]. The attained k_{app} values were $7.1 \times 10^{-4} \pm 2.8 \times 10^{-5}$ and $1.1 \times 10^{-3} \pm 8.7 \times 10^{-5}$ $cm\,s^{-1}$ for *f*MWCNT/GCE and CoPc-*f*MWCNT/GCE, respectively. These results clearly reflected the faster electron transfer process at CoPc-*f*MWCNT. Up to now, the effects of MWCNT and metallic phthalocyanine are still not fully understood and further studies are needed to clarify the electronic properties of these hybrid materials and accurately establish a correlation between these properties and the electrocatalytic behavior [56]. Also, studies performed by CV between 20 to $100\,mV\,s^{-1}$ (in 1.0×10^{-3} mol dm^{-3} $Fe(CN)_6^{4-}/Fe(CN)_6^{3-}$ (1:1) in 0.1 mol dm^{-3} KCl) showed a linear relationship between the peak currents and the square root of scan rate ($I_{p(anodic)}/A = 1.24 \times 10^{-7} \pm 2.89 \times 10^{-8} + 2.96 \times 10^{-5} \pm 1.14 \times 10^{-7}$ $\nu^{1/2}/V^{1/2}\,s^{-1/2}$, n = 4, R = 0.999; $I_{p(cathodic)}/A = -3.97$ $10^{-7} \pm 4.98 \times 10^{-8} - 2.81 \times 10^{-5} \pm 5.08 \times 10^{-7}$ $\nu^{1/2}/V^{1/2}\,s^{-1/2}$, n = 4, R = 0.999) suggesting a diffusion-controlled process.

3.2. Electrochemical behavior of FMT at CoPc-*f*MWCNT/GCE

CV experiments were performed from 0 to +1.5 V in order to characterize the electrochemical behavior of FMT at CoPc-*f*MWCNT/GCE (Fig. 4). The first scan at CoPc-*f*MWCNT/GCE revealed an irreversible oxidation process at *ca.* 1.2 V (a_0), and

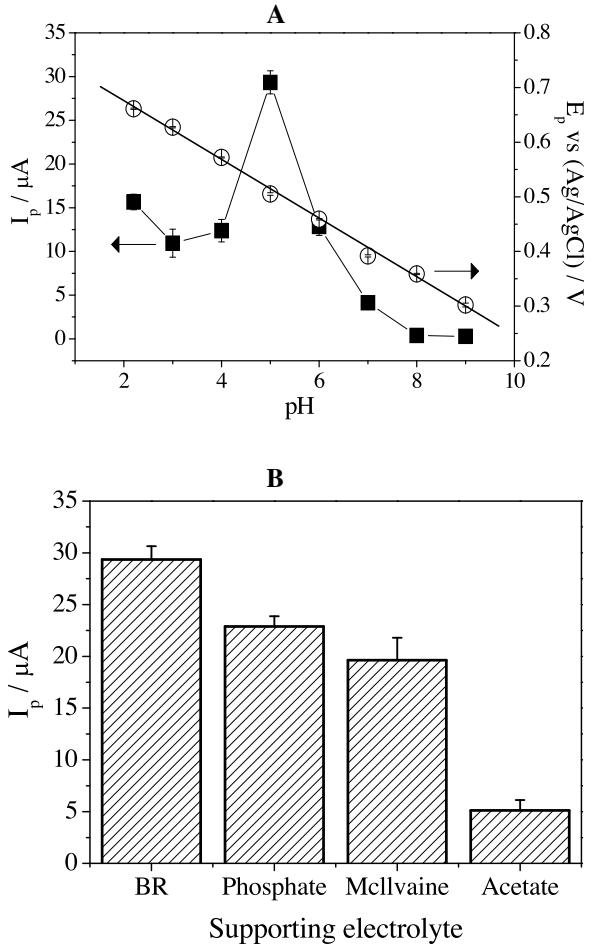

Fig. 5. (A) Influence of pH on 1.0×10^{-5} mol dm^{-3} FMT peak current (left y-axis) and peak potential (right y-axis) using CoPc-*f*MWCNT/GCE in Britton-Robinson (BR) buffer (0.04 mol dm^{-3}); (B) Effect of supporting electrolyte (pH 5.0; 0.04 mol dm^{-3}) on 1.0×10^{-5} mol dm^{-3} FMT peak current. Square-wave voltammetric parameters: accumulation potential 1.55 V, accumulation time 15 s, frequency $100\,s^{-1}$, amplitude 50 mV and step 2 mV.

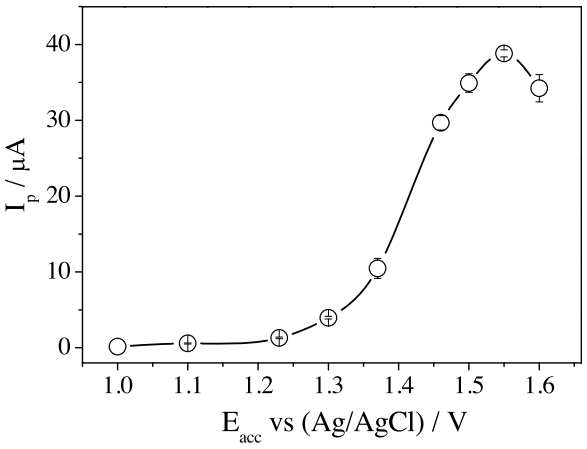

Fig. 6. Influence of accumulation potential on 1.0×10^{-5} mol dm^{-3} FMT peak current (t_{acc} = 15 s) at CoPc-*f*MWCNT/GCE (Britton-Robinson buffer pH 5.0). Square-wave voltammetric parameters: frequency 100 s^{-1}, amplitude 50 mV and step 2 mV.

two reduction peaks at *ca.* 0.50 V (c_1) and 0.35 V (c_2). In the subsequent scans, two anodic peaks appeared at 0.55 V (a_1) and 0.26 V (a_2). The redox peak couple a_2/c_2 matches to a reversible two-electron process (ΔE_p = 33.7 mV), and a_1/c_1 to a quasi-reversible process (ΔE_p = 126.9 mV). No peak was observed when CV assays were made in the range of 0.0 V to 0.8 V demonstrating that the set of peaks a_1/c_1 and a_2/c_2 are dependent of the a_0 process. This behavior is consistent with a three-step reaction of the electrochemical, chemical, electrochemical (ECE) mechanistic type, where a fast chemical reaction is interposed between two electron-transfer reactions (Scheme 2). It is known that the primary charge-transfer step of carbamates is one electron oxidation of the dimethylamino nitrogen attached to the conjugated system [57–59]. Thus the a_0 peak is probably due to the formation of the cation radical species which is unstable and undergo immediate hydrolysis; the new formed species (quinone-imine intermediate (I) and hydroxy-1,4-benzoquinone (II); Scheme 2) are then reduced and oxidized in the potential range 0.1 to 0.6 V. Preliminary adsorptive SWV experiments for FMT at CoPc-*f*MWCNT/GCE (using E_{acc} = 1.55 V, t_{acc} = 5 s, f = 100 s^{-1}, a = 50 mV, and ΔE_s = 2 mV) exhibited one more redox couple at *ca.* 0.20 V (a_3/c_3) than those recorded at CV assays (Fig. 4). This peak set (a_3/c_3) was clearly noticed because of the superior sensitivity of SWV and may be due to some other reaction intermediate of the first oxidation process. Still, from the third cyclic voltammogram, a poorly defined redox process seems to appear near a2/c2 (Fig. 4).

Since the pH affects the protonation mechanism involved in the ECE reaction, the dependence of the electrochemical response of the redox couple that showed the highest sensitivity (a_1/c_1) at CoPc-*f*MWCNT/GCE was studied over a pH range of 2.2 to 9.0 (0.04 mol dm^{-3} BR buffer) (Fig. 5A). The data showed that the peak current and potential are strongly pH dependent. The maximum peak current was clearly evidenced at pH 5.0, which was selected as the optimum value. Moreover, the peak potential (E_p) shifted towards more negative values as the pH increased. Using the experimental data (Ep *vs.* pH), the following equation was reached E_p (V) = 0.782 (V) − 0.054 pH (V/pH) (R = 0.9983; n = 8). The slope (∂Ep/∂pH) value is close to the theoretical value predicted by the Nernst equation (0.059 V/pH) indicating that an equal number of proton and electrons are involved in this electrochemical system [60]. The same conclusion was reached for the influence of pH on the irreversible oxidation process at *ca.* 1.2 V (a_0), and the obtained slope (∂Ep/∂pH) was 67.8 mV/pH. No potential shift was observed for pH higher than 8.0 since FMT has a pKa of 8.1 [61]. The highest peak current for a_0 was detected at pH 6.0. Regarding the influence of pH on the redox peak couple a_2/c_2, the maximum peak current was reached at pH 2.2, and no linear relation between the pH and the peak potential was perceived.

The effect of the supporting electrolyte on the electrochemical FMT peak current was also evaluated using four different buffers (at 0.04 mol dm^{-3}) namely acetate, BR, McIlvaine, and phosphate at the optimum pH value (Fig. 5B). It is known that the composition of the supporting electrolyte influences the conductivity, structure of the electrical double layer, kinetics of the electrochemical processes and diffusion coefficient [60]. The following order was established: I_p (BR) > I_p (phosphate) > I_p (McIlvaine) > I_p (acetate). BR buffer was further used as the electrolyte for FMT quantification.

3.3. Electroanalysis of FMT at CoPc-*f*MWCNT/GCE

3.3.1. Optimization of the square-wave voltammetric analysis

The combination of adsorptive stripping with SWV technique offers highly sensitive schemes for quantification of organic and inorganic compounds [62]. Furthermore, extremely low detection limits can be attained when coupling the adsorptive stripping accumulation with electrocatalysis. The influence of the accumulation potential (1.0 to 1.6 V) on the current of the redox couple a_1/c_1 at CoPc-*f*MWCNT/GCE was assessed (Fig. 6). The peak current of a_1/c_1 was about 92% higher than those of the other two sets, therefore, the optimization of instrumental parameters for FMT at

Table 1
Calibration data (n = 22) obtained for FMT quantification by SWV experiments (f = 100 s^{-1}, a = 30 mV and ΔE_s = 2 mV) at the CoPc-*f*MWCNT/GCE.

Parameter	CoPc-*f*MWCNT/GCE
Linearity range/mol dm^{-3}	9.80×10^{-8} to 3.92×10^{-6}
Intercept/A	-6.02×10^{-7}
Slope/A mol^{-1} dm^3	3.51
$t_{calculated}$[a]	1.73
Confidence interval of intercept	$\pm 9.61 \times 10^{-8}$
Confidence interval of the slope	±0.495
Correlation coefficient	0.9982
SD of the intercept/A	1.1×10^{-8}
SD of the slope/A mol^{-1} dm^3	5.5×10^{-2}
LOD/mol dm^{-3}	9.7×10^{-8}
LOD/mg kg^{-1}	0.02
LOQ/mol dm^{-3}	3.2×10^{-7}
LOQ/mg kg^{-1}	0.08

[a] t—Coefficient of the Student's t distribution at the 95% confidence level.

CoPc-*f*MWCNT/GCE, as well as the subsequent FMT quantification, was based on a_1/c_1. As far as the effect of the accumulation potential (E_{acc}; range of 1.0 to 1.6 V selected based on the CV studies) on the peak height is concerned, it is evident from the data plotted in Fig. 6 that the highest current was reached using a deposition potential of 1.55 V (about 250 fold-increase when compared with the response at E_{acc} = 1.0 V) which was selected as the optimum. Concerning the influence of the accumulation time, no peak was detected when no deposition time (or potential) was applied. Accumulation during a 5 s step was employed in the further optimization assays since this time provided good signal enhancement, appropriate sensitivity and allowed fast FMT analysis.

To get the highest sensitivity, the instrumental SWV parameters (*f*, a and ΔE_s) were also optimized (in BR buffer pH 5.0). The *f* was ranged from 10 to 300 s^{-1}, *a* from 1 to 70 mV and ΔE_s from 1 to 8 mV. A linear positive dependence between *f* and I_p values was obtained for the a_1/c_1 and a_3/c_3 couples in the range from 10 to

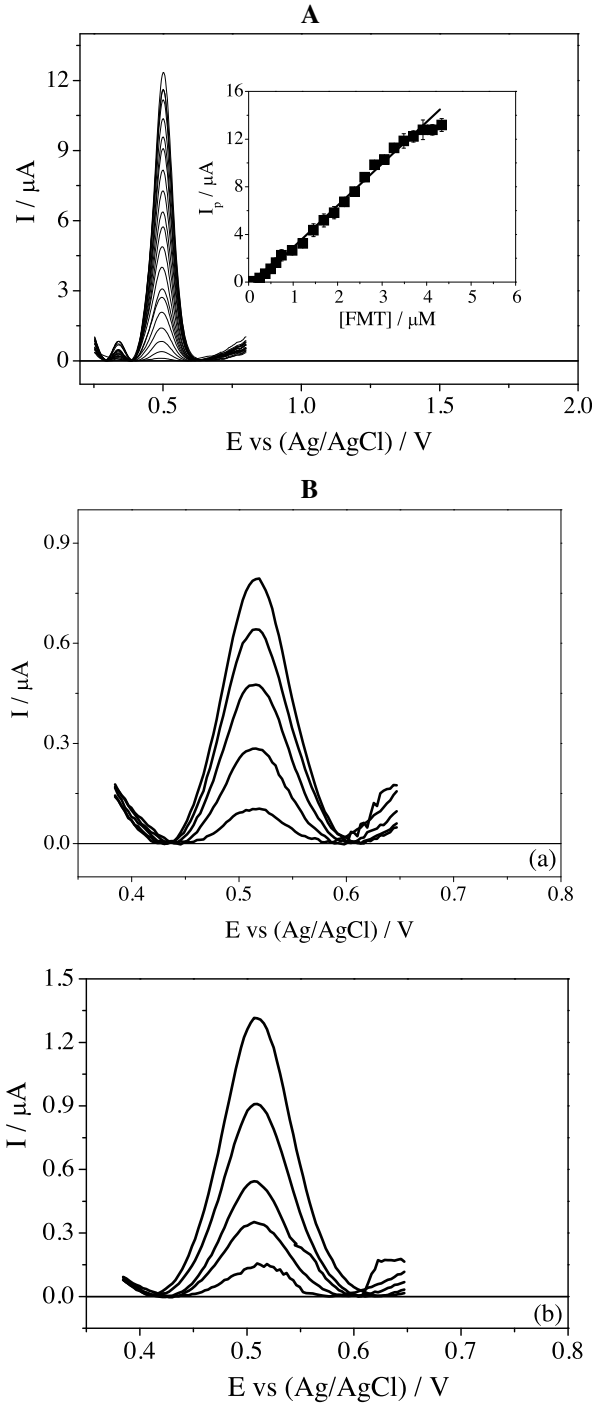

Fig. 7. (A) Square-wave voltammograms after successive standard additions of FMT (9.80×10^{-8} to 3.92×10^{-6} mol dm^{-3}) on CoPc-*f*MWCNT/GCE in Britton-Robinson buffer (pH 5.0). The inserts correspond to the respective FMT analytical curve. (B) Representative square-wave voltammograms obtained with CoPc-*f*MWCNT/GCE for FMT quantification in spiked (0.13 mg kg^{-1}) extracts of mango (a) and grape (b) samples (re-dissolved with Britton-Robinson buffer at pH 5.0) by the standard addition method. Square-wave voltammetric parameters: accumulation potential 1.55 V, accumulation time 5 s, frequency 100 s^{-1}, amplitude 30 mV and step 3 mV.

$100\,s^{-1}$. According to the theoretical model proposed by Lovrić et al. [63] for SWV, this type of relation indicates an adsorption-controlled process, which is characteristic of a surface redox reaction. Furthermore, no linear correlation was detected between E_p and log *f* which evidenced the quasi-reversible nature of the redox process (as already observed in the CV experiments discussed in section 3.2) [64]. The quasi-reversibility of the processes was also confirmed by the dependence between I_p/f and *f*. According to Komorsky-Lovrić and Lovrić [65,66], the maximum in the parabola (f_{max}/s^{-1}) is called the "quasi-reversible maximum" and can be used to estimate the standard rate constant (k_s/s^{-1}). It depends on the α (charge transfer coefficient) and *a* values, and can be calculated by equation (2):

$$k_s = k_{max} \times f_{max} \quad (2)$$

where k_{max} is the theoretically calculated critical kinetic parameter. When $0.25 \leq \alpha \leq 0.85$, the k_{max} value is 1.18 ± 0.05 [63]. The estimated quasi-reversible maxima were found to be $20\,s^{-1}$ for a_3/c_3 and $70\,s^{-1}$ for a_1/c_1. Thus, the attained k_s were $23.6 \pm 1.0\,s^{-1}$ and $82.6 \pm 3.5\,s^{-1}$ for a_3/c_3 and a_1/c_1, respectively. These values prove that the charge transfer kinetic is faster for the a_1/c_1 process which is in agreement with the higher current observed.

On the other hand, the a_2/c_2 process demonstrated a linear dependence between E_p and log *f*, and the half-peak width ($\Delta E_{p/2}$) was independent of *f*. This behavior is characteristic of a reversible reaction with adsorption of reagents [63]. In this case, the expression (3):

$$\Delta E_{p/2}/n = 101\ mV \quad (3)$$

can be applied to calculate the number of electrons (n) involved in the reaction. The attained value for $\Delta E_{p/2}$ was 48.4 mV (obtained with $f = 100\,s^{-1}$, $a = 50$ mV and $\Delta E_s = 2$ mV) indicating that two electrons participate in the electrochemical reaction.

The results revealed that $f = 100\,s^{-1}$, $a = 30$ mV and $\Delta E_s = 3$ mV originate the best signal-to-background current characteristics for the determination of FMT.

3.3.2. Analytical data

The optimal adsorptive square-wave voltammetric parameters were employed to obtain the calibration data for FMT using CoPc-*f*MWCNT/GCE (Table 1). The analytical curve (Fig. 7A) presented wide linearity and low dispersion of the data, even at low concentrations, with correlation coefficient (r) of 0.9982 (Table 1). High sensitivity (expressed by the slope of the analytical curve) was also observed ($3.51\,A\,mol^{-1}\,dm^3$; Table 1). The detection (LOD) and quantification limits (LOQ) were calculated using the standard deviation of the intercept and the average of slope of the straight line from the analytical curve [67]. Low LOD ($9.7 \times 10^{-8}\,mol\,dm^{-3}$; $0.02\,mg\,kg^{-1}$ (w/w)) and LOQ ($3.2 \times 10^{-7}\,mol\,dm^{-3}$; $0.08\,mg\,kg^{-1}$ (w/w)) were attained. The LOD calculated on a fresh weight basis is enough for application of the methodology to residue monitoring purposes in fruits and vegetables, considering the established Brazilian MRLs [33]. FMT is extensively applied for the protection of fruit and vegetable crops with MRLs ranging from 0.02 (mango) to $1.0\,mg\,kg^{-1}$ (w/w) (grapes) in fruits, and 0.05 (potato) to $2.0\,mg\,kg^{-1}$ (w/w) (pepper) in vegetables [33]. Nevertheless, if needed (the MRLs established in EU are lower for fruits and vegetables; 0.01 (mango) to 0.1 (grapes) [68]), a significant enhancement in LOD can be achieved by increasing the sample weight to be extracted and/or redissolving the crop residue in a lower volume of supporting electrolyte. Studies regarding the FMT electrochemical determination are scarce [29–32], none based on detection by MPc-MWCNT modified electrodes. The LOD achieved with the developed CoPc-*f*MWCNT/GCE is similar [30,32] or compares favorably with those reported previously for this pesticide based on more complex platforms [31].

Additionally, the (intra- and inter-day) repeatability and reproducibility was estimated at a controlled FMT concentration of $9.80 \times 10^{-7}\,mol\,dm^{-3}$. No significant differences were found between intra–day (n = 6) and inter–day experiments (n = 9) with relative standard deviations (RSD) ranging between 4.0 and 5.6%. The reproducibility of the CoPc–*f*MWCNT/GCE was also assessed using three different modified electrodes and the attained RSD was 2.4%. Overall, the proposed procedure exhibits appropriate features for analytical purposes.

3.4. Application to fruit samples

The accuracy and applicability of the proposed methodology were assessed by recovery assays of fortified mango and grape samples at four spiking levels ($0.13–0.73\,mg\,kg^{-1}$ (w/w)). No interference peaks were detected in the extract after the sample pretreatment (the residue was re-dissolved with the supporting electrolyte, BR buffer at pH 5.0) in the absence of FMT. The results are summarized in Table 2 and representative voltammograms are presented in Fig. 7B. Global average recoveries within the studied concentration ranges were 99%. More specifically, recoveries ranged from 98.0 ± 2.9 to 105.7 ± 1.8% for mango, and 94.2 ± 4.5% to 100.6 ± 1.5% for grape demonstrating the good accuracy and precision (RSDs ≤ 6.4%) of the electroanalytical procedure. These results confirm the practical utility of proposed method for FMT analysis in fruit matrices. Still, comparison of these results with those attained by the well-established technique, liquid chromatography tandem mass spectrometry (LC-MS/MS), would be precious to fully validate the developed electroanalytical procedure.

4. Conclusions

Although efforts are being made globally and a significant progress is being accomplished, the impact of carbamates on human and environmental health still remains a public health problem and an analytical challenge. Continuous efforts to develop reliable sensing tools are mandatory to mitigate dietary and

Table 2
Recovery of formetanate hydrochloride from spiked mango and grape samples (n = 3) using the CoPc-*f*MWCNT/GCE.

CoPc-*f*MWCNT/GCE					
	$[FMT]_{added}/mg\,kg^{-1}$	0.13	0.25	0.38	0.73
Mango	$[FMT]^a_{found}/mg\,kg^{-1}$	0.13 ± 0.02	0.24 ± 0.02	0.37 ± 0.01	0.77 ± 0.03
	Recovery/%	102.8	98.0	100.7	105.7
	RSD/%	6.4	2.9	1.3	1.8
Grape	$[FMT]^a_{found}/mg\,kg^{-1}$	0.12 ± 0.01	0.25 ± 0.01	0.35 ± 0.02	0.72 ± 0.02
	Recovery/%	94.2	100.6	94.2	99.2
	RSD/%	4.5	1.5	2.0	0.9

[a] mean ± confidence interval (based on Student's t distribution at 95% confidence level).

environmental risks. In that regard, the present work demonstrated that the voltammetric quantification of FMT in fruit samples can be successfully accomplished using the developed CoPc-*f*MWCNT/GCE. Considerable positive effects on the current signal were attained by combining the advantages of CoPc and *f*MWCNT (solubilized in Nafion®). The electrochemical behavior of FMT at CoPc-*f*MWCNT/GCE was consistent with an ECE mechanism. Globally, the proposed electrochemical device presents interesting characteristics, such as simplicity of preparation, short time of analysis, satisfactory sensitivity, accuracy, repeatability and reproducibility, being simultaneously environmental friendly and low-cost in comparison with the traditional chromatographic techniques used for residue determination. Also, the method yielded a LOD value lower than the established MRLs in fruits. Thus, it can constitute a reliable and independent alternative for food safety control.

Acknowledgements

The authors wish to thank the Brazilian research funding institution CNPq for their financial support through the project CNPq–PVE 2014 (Proc. 400223/2014-7 and 303596/2014-7). Francisco W. P. Ribeiro and Francisco W. de Souza Lucas also thank the São Paulo Research Foundation (FAPESP) for the grants 2012/10947-2, 2014/06704-2, INCTMN 2008/57872-1 and CNPq 573636/2008-7.

References

[1] E. Corsini, M. Sokooti, C.L. Galli, A. Moretto, C. Colosio, Pesticide induced immunotoxicity in humans: A comprehensive review of the existing evidence, Toxicology 307 (2013) 123.
[2] R.P. Keigwin, EPA-HQ-OPP-2010-0939: Formetanate HCl Final Work Plan for Registration Review June 2011, http://www.regulations.gov/#!documentDetail;D=EPA-HQ-OPP-2010-0939-0012 (accessed June 2015).
[3] J. Fisher, H. Dejmkova, J. Barek, Electrochemistry of pesticides and its analytical applications, Curr. Org. Chem. 15 (2011) 2923.
[4] O.D. Renedo, M.A.A. Lomillo, M.J.A. Martínez, Recent developments in the field of screen-printed electrodes and their related applications, Talanta 73 (2007) 202.
[5] F.W.P. Ribeiro, J.E.S. Soares, H. Becker, D. De-Souza, P. De Lima-Neto, A.N. Correia, Electrochemical mechanism and kinetics studies of haloperidol and its assay in commercial formulations, Electrochim. Acta 56 (2011) 2036.
[6] A. Chen, B. Shah, Electrochemical sensing and biosensing based on square-wave voltammetry, Anal. Method. 5 (2013) 2158.
[7] K. Scida, P.W. Stege, G. Haby, G.A. Messina, C.D. García, Recent applications of carbon-based nanomaterials in analytical chemistry: Critical review, Anal. Chim. Acta 691 (2011) 6.
[8] C. Gao, Z. Guo, J.H. Liu, X.J. Huang, The new age of carbon nanotubes: An updated review of functionalized carbon nanotubes in electrochemical sensors, Nanoscale 4 (2012) 1948.
[9] C.B. Jacobs, M.J. Peairs, B.J. Venton, Review: Carbon nanotube based electrochemical sensors for biomolecules, Anal. Chim. Acta 662 (2010) 105.
[10] X. Zhang, H. Ju, J. Wang, Electrochemical sensor, biosensor and their biomedical applications, Academic press, USA, 2008.
[11] F.C. Moraes, L.H. Mascaro, S.A.S. Machado, C.M.A. Brett, Direct electrochemical determination of glyphosate at copper phthalocyanine/multiwalled carbon nanotube film electrodes, Electroanal. 22 (2010) 1586.
[12] J. Wang, M. Musameh, Y. Lin, Solubilization of carbon nanotubes by Nafion toward the preparation of amperometric biosensors, J. Am. Chem. Soc. 125 (2003) 2408.
[13] J.H. Zagal, S. Griveau, J.F. Silva, T. Nyokong, F. Bedioui, Metallophthalocyanine-based molecular materials as catalysts for electrochemical reactions, Coordin. Chem. Rev. 254 (2010) 2755.
[14] H. Yin, Y. Zhou, J. Xu, S. Ai, L. Cui, L. Zhu, Amperometric biosensor based on tyrosinase immobilized onto multiwalled carbon nanotubes-cobalt phthalocyanine-silk fibroin film and its application to determine bisphenol A, Anal. Chim. Acta 659 (2010) 144.
[15] S. Nyoni, T. Mugadza, T. Nyokong, Improved l-cysteine electrocatalysis through a sequential drop dry technique using multi-walled carbon nanotubes and cobalt tetraaminophthalocyanine conjugates, Electrochim. Acta 128 (2014) 32.
[16] S. Nyoni, T. Nyokong, Electrocatalytic behaviour of cobalt tetraamino-phthalocyanine in the presence of a composite of reduced graphene nanosheets and of multi-walled carbon nanotubes, Electrochim. Acta 136 (2014) 240.
[17] C. Karuppiah, R. Devasenathipathy, S.M. Chen, D. Arulraj, S. Palanisamy, V. Mani, V.S. Vasantha, Fabrication of nickel tetrasulfonated phthalocyanine functionalized multiwalled carbon nanotubes on activated glassy carbon electrode for the detection of dopamine, Electroanalysis 27 (2015) 485.
[18] G. Bottari, D.D. Díaz, T. Torres, Alkynyl-substituted phthalocyanines: versatile building blocks for molecular materials synthesis, J. Porphyr. Phthalocya. 10 (2006) 1083.
[19] C.G. Claessens, W.J. Blau, M. Cook, M. Hanack, R.J.M. Nolte, T. Torres, D. Wöhrle, Phthalocyanines and phthalocyanine analogues: The quest for applicable optical properties, Monatsh. Chem. 132 (2011) 3.
[20] K.D. Wael, A. Adriaens, Comparison between the electrocatalytic properties of different metal ion phthalocyanines and porphyrins towards the oxidation of hydroxide, Talanta 74 (2008) 1562.
[21] S. Laschi, D. Ogończyk, I. Palchetti, M. Mascini, Evaluation of pesticide-induced acetylcholinesterase inhibition by means of disposable carbon-modified electrochemical biosensors, Enzyme Microb. Tech. 40 (2007) 485.
[22] G. Valdés-Ramírez, D. Fournier, M.T. Ramírez-Silva, J.L. Marty, Sensitive amperometric biosensor for dichlorovos quantification: Application to detection of residues on apple skin, Talanta 74 (2008) 741.
[23] G. Valdés-Ramírez, M. Cortina, M.T. Ramírez-Silva, J.L. Marty, Acetylcholinesterase-based biosensors for quantification of carbofuran, carbaryl, methylparaoxon, and dichlorvos in 5% acetonitrile, Anal. Bioanal. Chem. 392 (2008) 699.
[24] R.K. Mishra, R.B. Dominguez, S. Bhand, R. Muñoz, J.L. Marty, A novel automated flow-based biosensor for the determination of organophosphate pesticides in milk, Biosens. Bioelectron. 32 (2012) 56.
[25] M.P. Siswana, K.I. Izoemena, T. Nyokong, Electrocatalysis of asulam on cobalt phthalocyanine modified multi-walled carbon nanotubes immobilized on a basal plane pyrolytic graphite electrode, Electrochim. Acta 52 (2006) 114.
[26] F.C. Moraes, L.H. Mascaro, S.A.S. Machado, C.M.A. Brett, Direct electrochemical determination of carbaryl using a multi-walled carbon nanotube/cobalt phthalocyanine modified electrode, Talanta 79 (2009) 1406.
[27] M.P. Siswana, K.I. Ozoemena, D.A. Geraldo, T. Nyokong, Nanostructured nickel (II) phthalocyanine–MWCNTs as viable nanocomposite platform for electrocatalytic detection of asulam pesticide at neutral pH conditions, J. Solid State Electrochem. 14 (2010) 1351.
[28] L.J. Kong, M.F. Pan, G.Z. Fang, X.L. He, Y.Q. Xia, S. Wang, Electrochemical sensor based on a bilayer of PPY–MWCNTs–BiCoPc composite and molecularly imprinted PoAP for sensitive recognition and determination of metolcarb, RCS Adv. 5 (2015) 11498.
[29] M. Subbalakshmamma, S.J. Reddy, Electrochemical behavior of formetanate and chlordimefor pesticides, Electroanal. 6 (1994) 612.
[30] T.M.B.F. Oliveira, M.F. Barroso, S. Morais, M. Araújo, C. Freire, A.N. Correia, P. De Lima-Neto, M.B.P.P. Oliveira, C. Delerue-Matos, Laccase-Prussian blue film-graphene doped carbon paste modified electrode for carbamate pesticides quantification, Biosens. Bioelectron. 47 (2013) 292.
[31] T.M.B.F. Oliveira, M.F. Barroso, S. Morais, M. Araújo, C. Freire, P. De Lima-Neto, A.N. Correia, M.B.P.P. Oliveira, C. Delerue-Matos, Sensitive bi-enzymatic biosensor based on polyphenoloxidases–gold nanoparticles–chitosan hybrid film–graphene doped carbon paste electrode for carbamates detection, Bioelectrochemistry 98 (2014) 20.
[32] F.W.P. Ribeiro, M.F. Barroso, S. Morais, S. Viswanathan, P. De Lima-Neto, A.N. Correia, M.B.P.P. Oliveira, C. Delerue-Matos, Simple laccase-based biosensor for formetanate hydrochloride quantification in fruits, Bioelectrochemistry 95 (2014) 7.
[33] ANVISA (Agência Nacional de Vigilância Sanitária, Brazil), Monographs of authorized pesticides, Accessed at http://portal.anvisa.gov.br/wps/wcm/connect/73813200474592869ab9de3fbc4c6735/F40.pdf?MOD=AJPERES (accessed May 2015)
[34] G. Lai, F. Yah, H. Ju, Dual signal amplification of glucose oxidase-functionalized nanocomposites as a trace label for ultrasensitive simultaneous multiplexed electrochemical detection of tumor markers, Anal. Chem. 81 (2009) 9730.
[35] N. Havens, P. Trihn, D. Kim, M. Luna, A.K. Wanekaya, A. Mugweru, Redox polymer covalently modified multiwalled carbon nanotube based sensors for sensitive acetaminophen and ascorbic acid detection, Electrochim. Acta 55 (2010) 2186.
[36] Y. Han, J. Zheng, S. Dong, A novel nonenzymatic hydrogen peroxide sensor based on Ag–MnO_2–MWCNTs nanocomposites, Electrochim. Acta 90 (2013) 35.
[37] European Council Directive 2002/63/CE,, Establishing community methods of sampling for the official control of pesticide residues in and on products of plant and animal origin and repealing Directive 79/700/EEC, Off. J. Eur. Communities (2002) L187/30.
[38] V.L. Podhorniak, A. Kamel, D.M. Rains, Determination of formetanate hydrochloride in fruit samples using liquid chromatography-mass selective detection or-tandem mass spectrometry, J. Agri. Food Chem. 58 (2010) 5862.
[39] M. Anastassiades, S.J. Lehotay, D. Stajnbaher, F.J. Schenck, Fast and easy multiresidue method employing acetonitrile extraction/partitioning and dispersive solid-phase extraction for the determination of pesticide residues in produce, J. AOAC Int. 86 (2003) 412.
[40] H. Khani, O. Moradi, Influence of surface oxidation on the morphological and crystallographic structure of multi-walled carbon nanotubes via different oxidants, J. Nanostructure Chem. 3 (2013) 73.
[41] F.C. Moraes, M.F. Cabral, L.H. Mascaro, S.A.S. Machado, The electrochemical effect of acid functionalisation of carbon nanotubes to be used in sensors development, Surf. Sci. 190 (2014) 990.
[42] M. Mirzaeian, A.M. Rashidi, M. Zare, R. Ghabezi, R. Lotfi, Mercaptan removal from natural gas using carbon nanotube supported cobalt phthalocyanine nanocatalyst, Journal of Natural Gas Science and Engineering 18 (2014) 439.

[43] Z. Yang, H. Pu, J. Yuan, D. Wan, Y. Liu, Phthalocyanines–MWCNT hybrid materials: Fabrication, aggregation and photoconductivity properties improvement, Chemical Physics Letters 465 (2008) 73.
[44] H. Gong, S.T. Kim, J.D. Lee, S. Yim, Simple quantification of surface carboxylic acids on chemically oxidized multi-walled carbon nanotubes, Appl. Surf. Sci. 266 (2013) 219.
[45] S.Z. Kang, D. Yin, X. Li, J. Mu, A facile preparation of multiwalled carbon nanotubes modified with hydroxyl groups and their high dispersibility in ethanol, Colloid Surface A 384 (2011) 363.
[46] B.P. Vinayan, R.I. Jafri, R. Nagar, N. Rajalakshmi, K. Sethupathi, S. Ramaprabhu, Catalytic activity of platinum-cobalt alloy nanoparticles decorated functionalized multiwalled carbon nanotubes for oxygen reduction reaction in PEMFC, Int. J. Hydrogen. Energ. 37 (2012) 412.
[47] Y. Wang, N. Hu, Z. Zhou, D. Xu, Z. Wang, Z. Yang, H. Wei, E.S. Kong, Y. Zhang, Single-walled carbon nanotube/cobalt phthalocyanine derivative hybrid material: preparation, characterization and its gas sensing properties, J. Mater. Chem. 21 (2011) 3779.
[48] H. Li, Z. Xu, K. Li, X. Hou, G. Cao, Q. Zhang, Z. Cao, Modification of multi-walled carbon nanotubes with cobalt phthalocyanine: effects of the templates on the assemblies, J. Mater. Chem. 21 (2011) 1181.
[49] A. Morozan, S. Campidelli, A. Filoramo, B. Jousselme, S. Palacin, Catalytic activity of cobalt and iron phthalocyanines or porphyrins supported on different carbon nanotubes towards oxygen reduction reaction, Carbon 49 (2011) 4839.
[50] I. Kruusenberg, L. Matisen, K. Tammeveski, Oxygen electroreduction on multi-walled carbon nanotube supported metal phthalocyanines and porphyrins in acid media, Int. J. Electrochem. Sci. 8 (2013) 1057.
[51] K. Lee, J. Lee, S. Kim, B. Ju, Single-walled carbon nanotube/Nafion composites as methanol sensors, Carbon 49 (2011) 787.
[52] H. Bi, Y. Li, S. Liu, P. Guo, Z. Wei, C. Lv, J. Zhang, X.S. Zhao, Carbon-nanotube-modified glassy carbon electrode for simultaneous determination of dopamine, ascorbic acid and uric acid: The effect of functional groups, Sens. Actuat. B-Chem. 171–172 (2012) 1132.
[53] R.C. Alkire, D.M. Kolb, J. Lipkowshi, P.N. Ross, Chemically modified electrodes, WILEY-VCH Verlag GmbH & Co. KGaA, Weinheim Germany, 2009.
[54] J. Pillay, K.I. Ozoemena, Electrochemical properties of surface-confined films of single-walled carbon nanotubes functionalised with cobalt(II) tetra-aminophthalocyanine: Electrocatalysis of sulfhydryl degradation products of V-type nerve agents, Electrochim. Acta 52 (2007) 2630.
[55] M. Gamero, F. Pariente, E. Lorenzo, C. Alonso, Nanostructured rough gold electrodes for the development of lactate oxidase-based biosensors, Biosens. Bioelectron. 25 (2010) 2038.
[56] J.H. Zagal, S. Griveau, M.S. Nelli, S.G. Granados, F. Bedioui, Carbon nanotubes and metalloporphyrins and metallophthalocyanines based materials for electroanalysis, J. Porphyr. Phthalocya. 16 (2012) 713.
[57] G.E. Batley, B.K. Afgan, Voltammetric analysis of some carbamate pesticides, J. Electroanal. Chem. 125 (1981) 437.
[58] D. Nematollahi, H. Shayani-Jam, M. Alimoradi, S. Niroomand, Electrochemical oxidation of acetaminophen in aqueous solutions: Kinetic evaluation of hydrolysis, hydroxylation and dimerization processes, Electrochim. Acta 54 (2009) 7407.
[59] S.I. Bailey, I.M. Ritchie, A cyclic voltammetric study of the aqueous electrochemistry of some quinones, Electrochim. Acta 30 (1985) 3.
[60] R.G. Compton, C.E. Banks, Understanding Voltammetry, World Scientific Publishing, London, 2007.
[61] Conclusion regarding the peer review of the pesticide risk assessment of the active substance formetanate. EFSA Scientific Report 69 (2006) 1, http://www.efsa.europa.eu/sites/default/files/scientific_output/files/main_documents/69r.pdf (Accessed November 2015).
[62] O.A. Farghaly, R.S.A. Hameed, A.H. Abu-Nawwas, Analytical application using modern electrochemical techniques, Int. J. Electrochem. Sci 9 (2014) 3287.
[63] M. Lovrić, Š.K. Lovrić, Square–wave voltammetry of an adsorbed reactant, J. Electroanal. Chem. 248 (1988) 239.
[64] V. Mirčeski, Š.K. Lovrić, M. Lovrić, Square Wave Voltammetry Theory and Application, Springer, Berlim, 2007.
[65] Š. Komorsky-Lovrić, M. Lovrić, Kinetic measurements of a surface-confined redox reaction, Anal. Chim. Acta 305 (1995) 248.
[66] V. Mirčeski, R. Gulaboski, B. Jordanoski, Š. Komorsky-Lovrić, Square-wave voltammetry of 5-fluorouracil, J. Electroanal. Chem. 490 (2000) 37.
[67] J.N. Miller, J.C. Miller, Statistics and Chemometrics for Analytical Chemistry, Pearson Prentice Hall, United Kingdom, 2005.
[68] EU pesticide residues database for all the EU-MRLs, Available at http://ec.europa.eu/food/plant/protection/pesticides/database (accessed January 2015).